

Structural, mechanical and electrical characterization of epoxy-amine/carbon black nanocomposites

Th. V. Kosmidou¹, A. S. Vatalis¹, C. G. Delides¹, E. Logakis², P. Pissis^{2*}, G. C. Papanicolaou³

¹Technological Educational Institute of West Macedonia, Laboratories of Physics and Materials Technology, 50100 Kila, Kozani, Greece

²National Technical University of Athens, Department of Physics, Zografou Campus, 15780 Athens, Greece

³University of Patras, Department of Mechanical and Aeronautical Engineering, Rio Patras 26500, Greece

Received 5 February 2008; accepted in revised form 30 March 2008

Abstract. This work presents an insight into the effect of preparation procedure and the filler content on both electrical and mechanical properties of a nanocomposite system. For the preparation of the nanocomposites diglycidyl ether of bisphenol A (DGEBA) was used with triethylenetetramine (TETA) as a curing agent. As fillers carbon black (CB) nanoparticles with size from 25 to 75 nm were used. The characterization was done using Dynamic Mechanical Analysis (DMA), Dielectric Relaxation Spectroscopy (DRS), Differential Scanning Calorimetry (DSC), Wide Angle X-ray Diffraction (WAXD) and electrical conductivity measurements. The dependence of the dynamic mechanical and dielectric parameters (E' , E'' , $\tan\delta$, ϵ' , ϵ'' , σ and T_g) is associated with the filler content and is controlled by the employed curing conditions. An increase in electrical conductivity, which is observed at about 1% w/w of carbon black, indicates the creation of conducting paths and is associated with the Maxwell Wagner Sillars (MWS) relaxation, probably due to the formation of aggregated microstructures in the bulk composite.

Keywords: nanocomposites, epoxy resin, carbon black, curing, glass transition

1. Introduction

Nanocomposites show properties different from bulk polymers because of the small size of the filler and the corresponding increase in the surface area [1–7]. It is well known that the composite properties can change dramatically with the dispersion state, geometric shape, surface properties, particle size, and particle size distribution. Because of the recent commercial availability of nanoparticles, there is an increasing interest in polymer nanocomposites. These composites exhibit substantial improvements in their mechanical properties, such as the strength, modulus, and dimensional stability, permeability to gases, water and hydrocarbons, thermal stability, flame retardancy, chemical resist-

ance, and electrical, dielectric, magnetic and optical properties [8–15].

The effect of the nanofillers in polymer composites on the glass transition (T_g) and the relaxation behaviour of the polymer matrix has been studied for different filler-resin composites. In some cases an increase in T_g is reported in literature [2–4, 7], but the opposite result is also possible [5]. An initial decrease in T_g followed by an increase, at higher filler loadings, was observed in epoxy/carbon nanotubes composites [11]. In many cases, the amount, the dispersion and the surface conditions of the nanoparticles play important role in the changes in T_g and the mechanical properties of the nanocomposites [2, 6, 7].

*Corresponding author, e-mail: ppissis@central.ntua.gr
© BME-PT and GTE

In epoxy nanocomposites (generally in thermoset nanocomposites) there is an additional difficulty, as compared to thermoplastic nanocomposites. The conditions of the nanocomposites curing (and consequently the results of it) are usually different from those of the pure epoxy, due to the participation of the nanoparticles on the crosslinking mechanism [16].

Epoxy resins are electrical insulators. In order to dissipate electrostatic charges and to prepare materials with antistatic properties conductive nanoparticles such as carbon are dispersed in the polymer matrix [17]. Conductive filler – insulating polymer composites become conductors when the filler content reaches a critical value and their electrical conductivity show a sharp increase (percolation threshold). Balancing electrical conductivity with desirable mechanical behavior is one of the largest challenges for the use of filled polymer nanocomposites in various applications.

In this work we focus on the effect of both the curing procedure and the filler content, on the glass transition and the electrical and mechanical behaviour of the system.

2. Experimental

2.1. Materials

The pre-polymer D.E.R.332 used in this study is diglycidyl ether of bisphenol A (DGEBA) supplied by Fluka SA, U.S.A. The hardener used was triethylenetetramine (TETA) supplied by Sigma Aldrich, U.S.A. The extra conductive carbon black (particle size 25–75 nm) was obtained from Degussa, Germany; the typical values of the materials properties are presented in Table 1. All the components of the system are commercial products and were used without purification.

Table 1. Typical values for the carbon black used

Iodine absorption	[mg/g]	1075	ASTM D1510
CTAB surface area	[m ² /g]	600	ASTM D3765
OAN*	ml/100 g	380	ASTM D2414
COAN**	ml/100 g	370	ASTM D3493
Ash content	[%]	0.3	ASTM D1506
Heating loss at packaging	[%]	0.2	ASTM D1509
Sieve residue, 325 mesh	[ppm]	20	ASTM D1514
Pour density	[g/dm ³]	130	ASTM D1513

*oil absorption number

**oil absorption number on compressed sample

2.2. Sample preparation and methods

2.2.1. Sample preparation

The DGEBA/TETA/CB nanocomposites were prepared by the dispersion of the determined amount of CB in a glass vessel. Prior to that procedure, the pre-polymer was heated at 40°C in order to decrease the viscosity. The stoichiometric amount of TETA was added to the DGEBA matrix, and then the mixture was mechanically stirred for 1 h at 2000 rpm and degassed under vacuum for 15 min. Finally, the mixture was sonicated for 30 min in order to break up the CB agglomerates [1] and degassed again. The homogeneous liquid was poured in rectangular shaped Teflon molds and the samples were cured at 60°C for 20 h. Some of the samples were subjected to a post-curing procedure at 150°C for 2 h.

The amount of the hardener in the material is 14 phr (per hundred resin) corresponding to the stoichiometric ratio for complete curing of the resin. Seven series of specimens were produced, each one with different filler content, starting from 0% filler (pure resin), 0.05, 0.1, 0.5, 0.7, 1 and 2% w/w.

2.2.2. Wide angle X-ray scattering

Wide angle X-ray diffraction (WAXD) data were collected in the range of 2θ from 5 to 65° by a Philips PW1965/20 powder diffractometer, with Bragg-Brentano (θ, 2θ) geometry, using non-monochromated CuK_α radiation (λ = 1.54051 Å). The reflected intensities were recorded as a function of the scattering angle (2θ). The size of the orientation regions *L* was calculated by the Scherrer's formula (1) [18]:

$$L = \frac{0.9\lambda}{\cos\theta \cdot \text{FWHM}} \quad (1)$$

where λ is the wavelength, θ is the position of the peak and FWHM the width in the middle of the peak.

2.2.3. Dynamic Mechanical thermal Analysis (DMA)

A Polymer Laboratories dynamic mechanical thermal analyzer MK III operating at a frequency of 10 Hz, a strain of 4× and a scanning rate of 2°C/min was used. Measurements were performed from

room temperature up to 200°C and the resultant changes in E' , E'' and $\tan\delta$ were plotted.

2.2.4. Differential Scanning Calorimetry (DSC)

A Perkin Elmer Differential Scanning Calorimeter (Pyris 6, DSC) was used under nitrogen atmosphere. The measurements were performed from room temperature to 200°C at a programmed heating rate of 20°C/min.

2.2.5. Dielectric measurements

With DRS analysis, the complex dielectric permittivity ($\epsilon^* = \epsilon' - i\epsilon''$, where ϵ' is the dielectric constant and ϵ'' is the dielectric loss) is measured as a function of frequency (10⁻²–10⁶ Hz) and temperature (from -150 to 200°C) [19–22]. An Alpha Analyser, in combination with a Quatro Cryosystem (Novocontrol, Germany), was used. Each sample was clamped between gold-plated, stainless steel electrodes in a Novocontrol dielectric cell. By measuring the complex impedance ($Z^* = Z' - iZ''$) of the circuit, the complex permittivity ($\epsilon^* = \epsilon' - i\epsilon''$) arises from Equation (2):

$$\epsilon^*(\omega) = \frac{1}{i\omega Z^*(\omega)C_0} \quad (2)$$

where ω is the angular frequency ($\omega = 2\pi f$) of the applied electric field and C_0 the equivalent capacitance of the free space.

2.2.6. Conductivity measurements

Using the complex permittivity data, the frequency-dependent ac electrical conductivity (real part, σ) is obtained from Equation (3):

$$\sigma = \epsilon'' \cdot \omega \cdot \epsilon_0 \quad (3)$$

where $\epsilon_0 = 8.85 \cdot 10^{-12} \text{ F} \cdot \text{m}^{-1}$ is the permittivity of free space.

3. Results and discussion

3.1. Morphological characterization

The WAXD spectra are shown in Figure 1. Epoxy nanocomposites were completely amorphous showing an amorphous halo at 19° of 2θ which is independent in position and magnitude from the filler content. This broad peak is probably attributed to

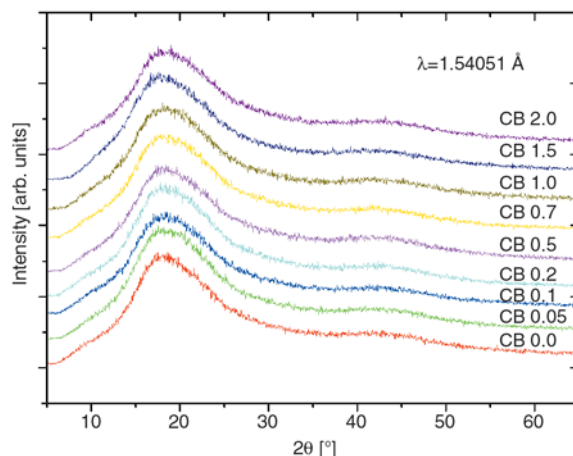


Figure 1. Wide angle X-ray diffraction patterns of DGEBA/TETA/CB nanocomposites

the formation of small clusters with some molecular orientation [18], the size of which is calculated from the Scherrer's formula (Equation (1)) to be about 8 Å. These regions of molecular order are consistent with the close alignment of the epoxy elements of the matrix which occurs when the bisphenol groups are able to close pack.

3.2. Mechanical properties

In the DGEBA/TETA/CB system, the components of the dynamic modulus and T_g are examined in two distinguished curing conditions (a: 60°C for 20 h stage 1 and b: 150°C for 2 h stage 2) as a function of the filler content.

Typical traces for the DMA of the unfilled resin and filled composites cured at 60 and 150°C are presented in Figures 2–5.

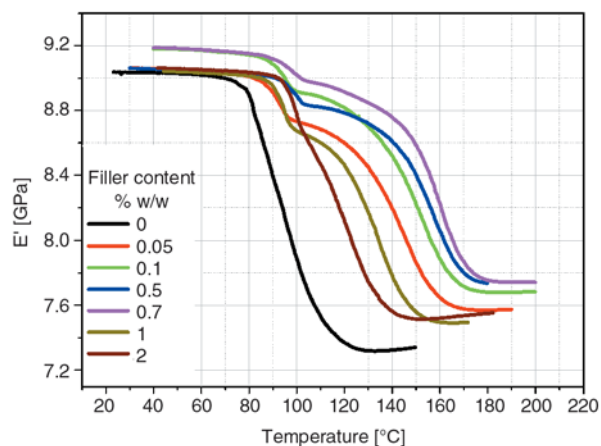


Figure 2. DMA spectra: E' as a function of temperature at frequency of 10 Hz. Curing conditions: 60°C, 20 h (non post-cured)

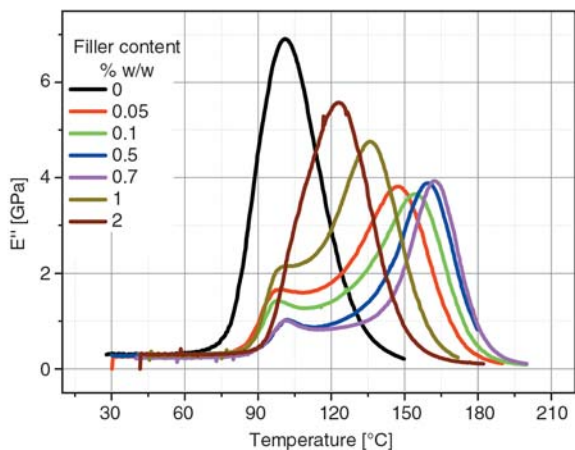


Figure 3. DMA spectra: E'' as a function of temperature at frequency of 10 Hz. Curing conditions: 60°C, 20 h (non post-cured)

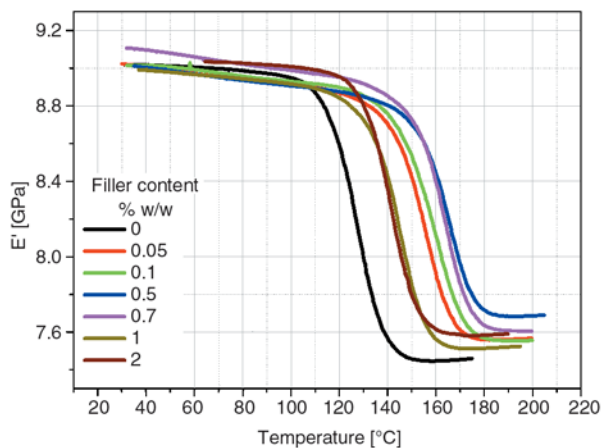


Figure 4. DMA spectra: E' as a function of temperature at frequency of 10 Hz. Curing conditions: 60°C, 20 h and 150°C, 2 h (post-cured)

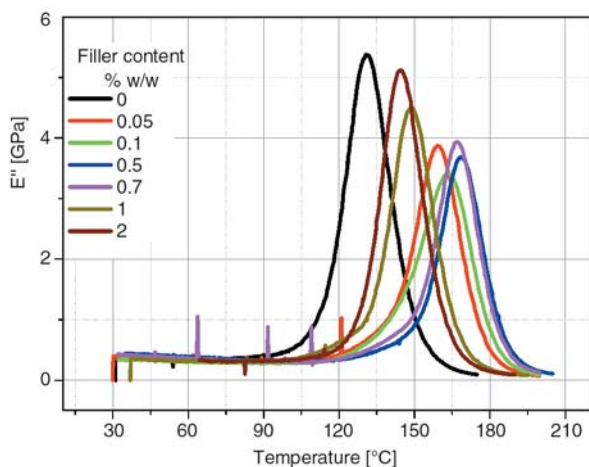


Figure 5. DMA spectra : E'' as a function of temperature at frequency 10 Hz. Curing conditions: 60°C, 20 h and 150°C, 2 h (post-cured)

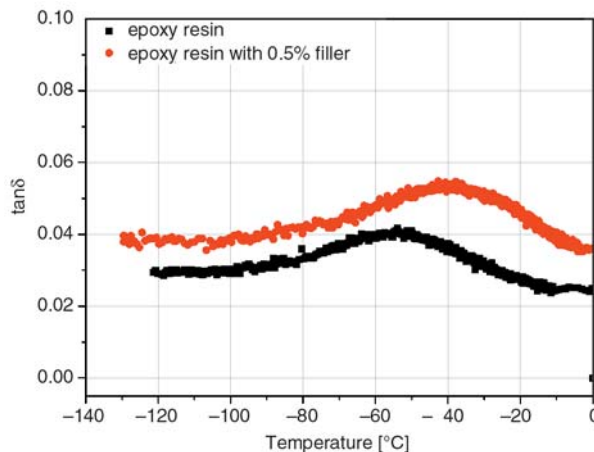


Figure 6. Low temperature DMA spectra: $\tan\delta$ as a function of temperature at frequency 10 Hz for pure resin and resin nanocomposite with 0.5% w/w CB

As it is clearly shown, E' is slightly affected by the filler content in the glassy state and increases significantly in the rubbery one. The T_g , which was determined as the temperature of $\tan\delta$ peak, increases with the curing temperature (for the pure epoxy T_g increases from 101°C up to the ultimate post-curing value of 131°C) due to further crosslinking of unreacted epoxy with the TETA amine groups. Also an additional relaxation is observed in the partially cured nanocomposites which will be discussed later.

Raw data of $\tan\delta$ for the pure resin and the nanocomposite with 0.5% CB content at subzero temperatures are shown in Figure 6. There is a small peak in $\tan\delta$ at about -55°C which corresponds to the secondary β -relaxation [23–25]. This peak shifts to higher temperatures (around -40°C) in the nanocomposite. Such a behavior is in agreement with dielectric relaxation spectroscopy results which are presented below and perhaps is an evidence for different curing procedure in the pure epoxy and in the nanocomposites.

3.3. Effect of curing procedure and filler content on T_g

The T_g dependence on the CB-content is presented in Figure 7 for the two distinctly different curing conditions (60°C, 20 h and 150°C, 2 h).

In both cases, at low filler contents, T_g increases up to a maximum value (at about 0.7% w/w) of filler content, and afterwards decreases. This dependence is similar in both groups of samples (before and

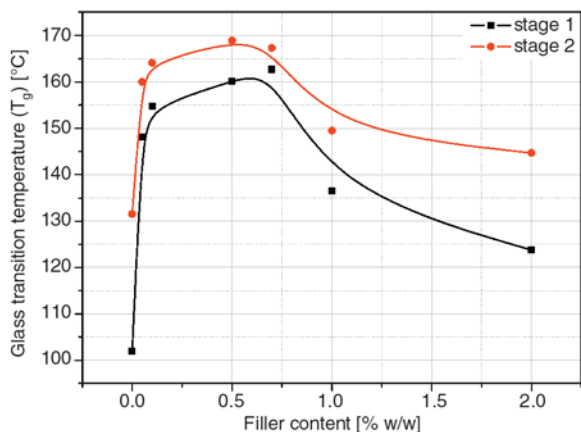


Figure 7. The dependence of T_g as a function of filler content at curing conditions (stage 1): 60°C, 20 h and (stage 2): 60°C for 20 h plus 150°C, 2 h

Table 2. Glass transition Temperatures for sub(T_{gs})- and post(T_{gp})-cured states

Filler content [wt%]	0.0	0.05	0.1	0.5	0.7	1.0	2.0
T_{gs} [°C]	102	110	115	160	142	137	124
T_{gp} [°C]	132	136	137	169	154	149	145
ΔT_g [°C]	30	26	22	9	12	17	21

after post-curing) and is confirmed also by DSC measurements. In Table 2 the glass transition temperatures for sub(T_{gs})- and post(T_{gp})-cured states and the difference $T_{gp} - T_{gs}$ are presented.

This unexpected behavior shows a remarkable difference with the predictions of the statistical theory available for randomly dispersed and distributed fillers. A similar behaviour was observed in poly(vinyl alcohol)/clay nanocomposites [26]. It can be qualitatively explained by the coexistence of the two mechanisms (namely interfacial constrains and free volume increase [20]) which can be responsible for the T_g shifting. In any nanocomposite the two mechanisms are in dynamic equilibrium. The equilibrium point depends on many factors (filler's amount, size, etc.) and in that way it analogically affects the T_g .

According to the first mechanism, a short-range, highly immobilized layer of a few nm thick is developed near the surface of the fillers. In this interaction region of the polymer layer surrounding the particles, the conformational entropy and the chains kinetics are significantly altered. As the filler content increases the volume fraction of the interaction region in the nanocomposites increases too. The polymer chains in this region are under constrain because of the interfacial polymer-parti-

cle interactions and therefore T_g of the nanocomposites has been shifted to higher temperatures.

Based on the concept of free volume, the increase of the filler content increases the free volume due to loosened molecular packing of the chains. This extra created free volume assists the large-scale segmental motion of the polymer. As a result, T_g of the nanocomposites decreases as the filler loading increases.

In our case, at low filler content the first mechanism (interfacial constrains) dominates and therefore contributes to a T_g increase with the filler loading. After a certain amount of filler (0.7% w/w) the second mechanism (free volume increase) starts to be dominant and the T_g decreases with the filler content.

This inversion in the domination of the mechanisms which are responsible to T_g shifting could be explained as a consequence of a transition of the filler arrangement within the matrix. The critical value of CB content separates, in fact, a dispersed and an agglomerated state and can therefore not be compared with the one obtained through a purely random geometrical process. The CB particles have permanent electrical charges at their surfaces, which are probably responsible for this morphological structure.

3.4. The new sub- T_g

As it is clearly shown in Figures 2 to 5 an additional relaxation is observed (a peak below and close to T_g and in the same temperature as for the pure resin) in the partially cured nanocomposites. This indicates the existence of two crosslinking mechanisms which act in these stages of curing. The first mechanism is caused by the reaction of the crosslink agent with the epoxy groups and the second one appears as a result of the filler's effect on the curing reaction, giving in that way the dominated α -relaxation.

The presence of this new relaxation in the sub-cured samples (60°C curing temperature) indicates that a formation of a resin-filler interphase takes place just before the full curing procedure is completed.

The development of short-range, highly immobilized layer near the surface of the filler with a thickness of about 2 nm has been reported in these systems [5–7]. In this interaction region of the

polymer layer which surrounds the particles, the conformational entropy and chain kinetics are significantly altered [5]. Due to the small size of the filler particle, the filler-matrix interphase is rapidly increased with filler content. This becomes the basis for potentially remarkable changes in the nanocomposite properties. In the post-cured composites the crosslink density increases tremendously, the interphase region reduces significantly and the sub- T_g relaxation disappears. Perhaps this could be attributed to the incorporation of the loose chains into the network.

3.5. The DRS and conductivity measurements

Molded samples of the DGEBA/TETA/CB system cured at 60°C for 20 h (non post-cured) were used for dielectric measurements. The samples were scanned in the DRS at room temperature in the frequency region from 10^{-2} to 10^6 Hz. The data were analyzed in terms of real part of dielectric permittivity (constant) ϵ' , imaginary part of dielectric permittivity (dielectric loss) ϵ'' and ac electrical conductivity σ . At low filler content, below 1% w/w, $\epsilon'(f)$ increases moderately in the composites with respect to the pure matrix (results shown in the inset to Figure 8). It is interesting to note that in this group of composites ϵ' decreases systematically with increasing filler content. This decrease is in very good agreement with the increase of the glass transition temperature T_g with increasing filler content in Table 2. Bearing in mind that $\epsilon'(f)$ reflects the ability of molecular dipoles connected

with the polymer chains for reorientation in the applied electric field, i.e. molecular mobility [27], these results can be understood as follows. With increasing filler content, molecular mobility in the composites decreases as a result of polymer-filler interactions. The decrease of molecular mobility is reflected as an increase of T_g in DSC and DMA measurements and as a concomitant decrease of $\epsilon'(f)$ in DRS measurements. This explanation does not apply for the pure matrix, which exhibits the lowest $\epsilon'(f)$ values and at the same time the lowest T_g (Table 2). Similar to other results reported above, by comparing data for the pure matrix with those for the composites we should keep in mind that curing in the composites occurs in the presence of the filler, i.e. curing conditions are different in the two cases. At higher filler contents, starting with 1%, a significant increase of $\epsilon'(f)$ is observed in Figure 8. The origin of that increase will be discussed in relation to $\epsilon''(f)$.

Experimental data of the imaginary part of the dielectric constant ϵ'' vs. frequency at room temperature are shown in Figure 9. In the first group of samples (pure matrix and composites with less than 1% CB) a relaxation (loss peak) is observed at about 10^5 Hz. Comparison with data in the literature indicates that this is the β -relaxation attributed to the crankshaft rotation of the hydroxyether group $[-CH_2-CH(OH)-CH_2-O-]$ generated by the reaction between epoxide and amino groups [2, 7, 16]. In the second group of composites, those with higher filler content, starting with 1%, an overall and significant increase of $\epsilon''(f)$ is observed. As a

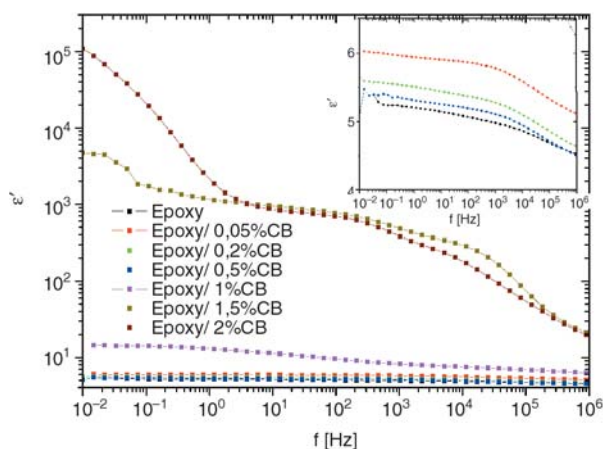


Figure 8. Real part of the dielectric permittivity (ϵ') versus frequency f at room temperature for the samples indicated on the plot. The inset shows details for the samples with low filler content

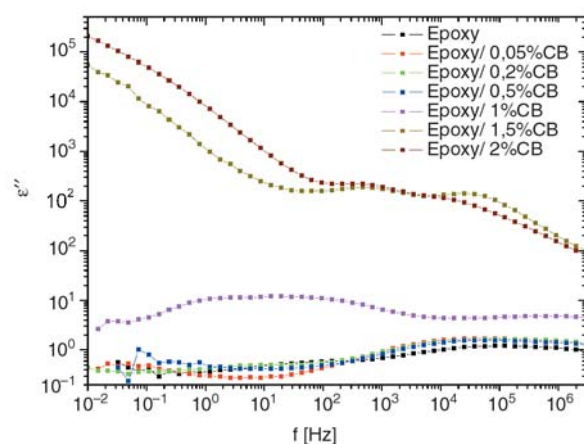


Figure 9. Imaginary part of the dielectric permittivity (ϵ'') versus frequency f at room temperature for the samples indicated on the plot

result, the β -relaxation is masked and can no more be followed. Please note the high values of $\epsilon'(f)$ for the same group of composites in Figure 8. In agreement with data reported for similar systems in the literature [7, 16], the large increase of both $\epsilon'(f)$ in Figure 8 and $\epsilon''(f)$ in Figure 9 is to a large extent related to the formation of a percolation structure of the nanoparticles, as confirmed by conductivity data in Figure 10 to be discussed later. Please note that the percolation structure, related with the formation of agglomerates in the bulk composite, is reflected also in the CB content dependence of the glass transition temperature T_g discussed in Section 3.3.

In addition to the overall increase of $\epsilon'(f)$ and $\epsilon''(f)$ in the composites with high CB content, a broad and complex relaxation is observed between 1 and 100 Hz for the sample with 1% CB content, which is shifted to higher frequencies at higher CB content. We think that this is Maxwell–Wagner–Sillars (MWS) relaxation, associated with the formation of agglomerates of CB [16]. It is reasonable to assume a broad distribution of size and conductivity of these agglomerates, which give rise to the broad and complex MWS relaxation observed. It is interesting to note that, as pointed out by one of the referees, $\epsilon'(f)$ goes to saturation at low frequencies for the sample with 1% CB, this result providing support for the attribution of the relaxation to MWS polarization. The same is true for the samples with higher CB content. The further increase of $\epsilon'(f)$ in these samples at even lower frequencies is attributed to space charge polarization [28].

Figures 10 and 11 show results for the electrical ac conductivity σ calculated from the measured

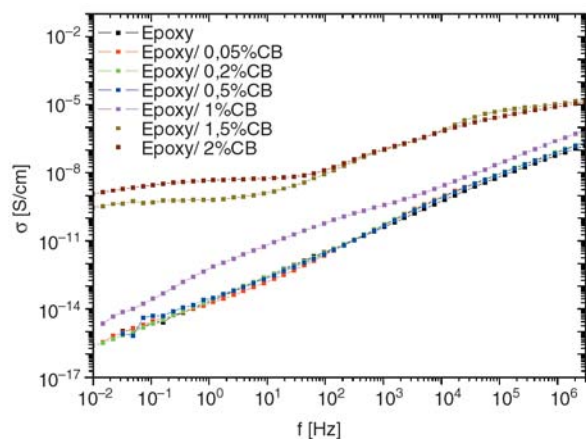


Figure 10. Electrical conductivity (σ) versus frequency f at room temperature for the samples indicated on the plot

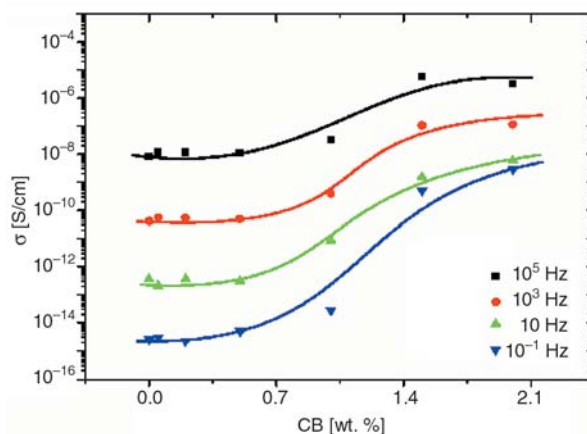


Figure 11. Electrical conductivity (σ) as a function of nanoparticle content at different frequencies indicated on the plot. The lines are guides for the eye

dielectric loss $\epsilon''(f)$ by using Equation (3). A typical dielectric behavior is observed below 1% CB (conductivity increases linearly with the frequency). At higher CB contents conductivity increases significantly and plateau values are observed at low frequencies for the composites with 1.5 and 2% CB. In consistency with the dielectric data presented in Figures 8 and 9 and discussed above, the large increase of conductivity in these samples is attributed to the formation of a percolation structure. Thus, the results suggest that in the system under investigation the percolation threshold is between 1.0 and 1.5 wt% CB. A final comment refers to the relatively low values of both the percolation threshold and the dc conductivity of the composites under investigation (dc conductivity 10^{-9} to 10^{-8} S/cm for the composite with 2 wt% CB), as compared to metal/polymer composites [29]. Please note, however, that similar values to those of the present work were reported in the past and recently [30] for various CB/polymer composites.

4. Conclusions

The dielectric and dynamic mechanical behaviour of epoxy/carbon black composite was systematically investigated. WAXD patterns show the existence of small, about 8 Å in size, orientated regions which are consistent with the close alignment of the epoxy elements of the matrix which occurs when the bis phenol groups are able to close pack.

The dependence of T_g on the filler content shows a peculiar behaviour. An increase up to a maximum, corresponding to about 0.7% w/w of CB, followed

by a decrease, with the appearance of a new relaxation below and close to T_g in the sub-cured samples is observed. The shift of the β -relaxation (associated to the crankshaft rotation of the hydrox-yether group) to higher temperature is an evidence for different curing between the pure epoxy and the nanocomposites.

The increase of the high temperature modulus (rubbery state) as the filler content increases indicates that the CB acts as classical filler and that the polymer interacts with the filler particles. The lack of significant increase in the low temperature modulus (glassy state) with the filler content is unexpected. This partially could be attributed to high degree of crosslink density of the matrix which covers the filler contribution.

The low dielectric constant below the filler content of 1% w/w indicates clearly that no cluster formation takes place and this filler content separates, in fact, the dispersed and the agglomerated state of nanoparticles.

A correlation between conductivity and glass transition behavior in epoxy resin based nanocomposites is observed.

Acknowledgements

This work has been funded by the projects 'Archimedes' and 'PENED'. PENED is co financed 75% of public expenditure through EC – European Social Fund, 25% of public expenditure through Ministry of Development – General Secretariat of Research and Technology and through private sector, under measure 8.3 of OPERATIONAL PROGRAMME 'COMPETITIVENESS' in the 3rd Community Support Programme. Acknowledgements are also expressed to Professor R. A. Pethrick for the stimulating discussions during this work and to student Vangelis Varsamidis for his contribution to sample preparation.

References

- [1] Sun Y., Zhang Z., Moon K-S., Wong C. P.: Glass transition and relaxation behavior of epoxy nanocomposites. *Journal of Polymer Science, Part B: Polymer Physics*, **42**, 3849–3858 (2004).
- [2] Brown J., Rhoney I., Pethrick R. A.: Epoxy resin based Nanocomposites: 1. Diglycidylether of bisphenol A (DGEBA) with triethylenetetramine (TETA). *Polymer International*, **53**, 2130–2137 (2004).
- [3] Cao Y. M., Sun J., Yu D. H.: Preparation and properties of nano- Al_2O_3 particles/ polyester/epoxy resin ternary composites. *Journal of Applied Polymer Science*, **83**, 70–77 (2002).
- [4] Pham J. Q., Mitchell C. A., Bahr J. L., Tour J. M., Krishnamoorti R., Green P. F.: Glass transition of polymer/single-walled carbon nanotube composite films. *Journal of Polymer Science, Part B: Polymer Physics*, **41**, 3339–3345 (2003).
- [5] Ash B. J., Schadler L. S., Siegel R. W.: Glass transition behavior of alumina/polymethylmethacrylate nanocomposites. *Materials Letters*, **55**, 83–87 (2002).
- [6] Xiong M., Gu G., You B., Wu L.: Preparation and characterization of poly(styrene butylacrylate) latex/nano-ZnO nanocomposites. *Journal of Applied Polymer Science*, **90**, 1923–1931 (2003).
- [7] Kotsilkova R., Fragiadakis D., Pissis P.: Reinforcement effect of carbon nanofillers in an epoxy resin system: Rheology, molecular dynamics, and mechanical studies. *Journal of Polymer Science, Part B: Polymer Physics*, **43**, 522–533 (2005).
- [8] Pelster R., Simon U.: Nanodispersions of conducting particles: Preparation, microstructure and dielectric properties. *Colloid and Polymer Science*, **277**, 2–14 (1999).
- [9] Krishnamoorti R., Giannelis E. P.: Rheology of end-tethered polymer layered silicate nanocomposites. *Macromolecules*, **30**, 4097–4102 (1997).
- [10] Reynaud E., Jouen T., Gauthier C., Vigier G., Varlet J.: Nanofillers in polymeric matrix: A study on silica reinforced PA6. *Polymer*, **42**, 8759–8768 (2001).
- [11] Berriot J., Montes H., Lequeux F., Long D., Sotta P.: Evidence for the shift of the glass transition near the particles in silica-filled elastomers. *Macromolecules*, **35**, 9756–9762 (2002).
- [12] Arrighi V., McEwen I. J., Qian H., Serrano Prieto M. B.: The glass transition and interfacial layer in styrene-butadiene rubber containing silica nanofiller. *Polymer*, **44**, 6259–6266 (2003).
- [13] Psarras G. C., Gatos K. G., Karahaliou P. K., Georga S. N., Krontiras C. A., Karger-Kocsis J.: Relaxation phenomena in rubber/layered silicate nanocomposites. *Express Polymer Letters*, **1**, 837–845 (2007).
- [14] Zhou Y. X., Wu P. X., Cheng Z-Y., Ingram J., Jeelani S.: Improvement in electrical, thermal and mechanical properties of epoxy by filling carbon nanotube. *Express Polymer Letters*, **2**, 40–48 (2008).
- [15] Bajpai A. K., Bajpai J., Soni S. N.: Preparation and characterization of electrically conductive composites of poly(vinyl alcohol)-g-poly(acrylic acid) hydrogels impregnated with polyaniline (PANI). *Express Polymer Letters*, **2**, 26–39 (2008).
- [16] Pissis P., Fragiadakis D.: Dielectric studies of segmental dynamics in epoxy nanocomposites. *Journal of Macromolecular Science: Physics*, **46**, 119–136 (2007).

- [17] Markov A., Fiedler B., Schulte K.: Electrical conductivity of carbon black/fibres filled glass-fibre-reinforced thermoplastic composites. *Composites, Part A: Applied Science and Manufacturing*, **37**, 1390–1395 (2006).
- [18] Guinier A.: X-ray diffraction in crystals, imperfect crystals and amorphous bodies. W. H. Freeman and Company, San Francisco (1963).
- [19] Krishnamoorti R., Vaia R., Giannelis E.: Structure and dynamics of polymer-layered silicate nanocomposites. *Chemistry of Materials*, **8**, 1728–1734 (1996).
- [20] Bershtein V. A., Egorova L. M., Yakushev P. N., Pissis P., Sysel P., Brozova L.: Molecular dynamics in nanostructured polyimide-silica hybrid materials and their thermal stability. *Journal of Polymer Science, Part B: Polymer Physics*, **40**, 1056–1069 (2002).
- [21] Kanapitsas A., Pissis P., Kotsilkova R.: Dielectric studies of molecular mobility and phase morphology in polymer-layered silicate nanocomposites. *Journal of Non-crystalline Solids*, **305**, 204–211 (2002).
- [22] Pissis P., Kanapitsas A., Georgoussis G., Bershtein V. A., Sysel P.: Dielectric studies of phase morphology and molecular mobility in novel nanocomposites based on polyimide. *Advanced Composites Letters*, **11**, 49–58 (2002).
- [23] Delides C. G., Hayward D., Pethrick R. A., Vatalis A. S.: Real time dielectric investigations of phase separation and cure in rubber modified epoxy resin systems. *European Polymer Journal*, **28**, 505–512 (1992).
- [24] Delides C. G., Hayward D., Pethrick R. A., Vatalis A. S.: Dielectric and morphological investigations of phase separation and cure in rubber-modified epoxy resins: Comparison between tetra- and DDM-based systems. *Journal of Applied Polymer Science*, **47**, 2037–2051 (1993).
- [25] Delides C. G., Vatalis A. S., Pissis P., Pethrick R. A.: Dielectric and thermally stimulated discharge current studies of rubber-modified epoxy resins. *Journal of Macromolecular Science: Physics*, **32**, 261–274 (1993).
- [26] Bandi S., Schiraldi D. A.: Glass transition behavior of clay aerogel/poly(vinyl alcohol) composites. *Macromolecules*, **39**, 6537–6545 (2006).
- [27] Runt J. P., Fitzgerald J. J.: Dielectric spectroscopy of polymeric materials. American Chemical Society, Washington (1997).
- [28] Kyritsis A., Pissis P., Grammatikakis J.: Dielectric relaxation spectroscopy in poly(hydroxyethyl acrylate)/water hydrogels. *Journal of Polymer Science, Part B: Polymer Physics*, **33**, 1737–1750 (1995).
- [29] Mamunya Y. P., Davydenko V. V., Pissis P., Lebedev E. V.: Electrical and thermal conductivity of polymers filled with metal powders. *European Polymer Journal*, **38**, 1887–1897 (2002).
- [30] Koysuren O., Yesil S., Bayram G.: Effect of composite preparation techniques on electrical and mechanical properties and morphology of nylon 6 based conductive polymer composites. *Journal of Applied Polymer Science*, **102**, 2520–2526 (2006).